

# Straightforward Access to Amphiphilic Dual Bottle Brushes by Combining RAFT, ATRP, and NMP Polymerization in One Sequence

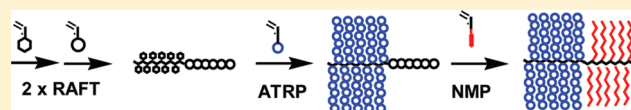
Daniel Zehm,<sup>†</sup> André Laschewsky,<sup>\*,†,‡</sup> Hua Liang,<sup>§</sup> and Jürgen P. Rabe<sup>§</sup>

<sup>†</sup>Institut für Chemie, Universität Potsdam, Karl-Liebknecht-Strasse 24-25, 14476 Potsdam-Golm, Germany

<sup>‡</sup>Fraunhofer Institut für Angewandte Polymerforschung, Geiselbergstrasse 69, 14476 Potsdam-Golm, Germany

<sup>§</sup>Department of Physics, Humboldt-Universität zu Berlin, Newtonstrasse 15, 12489 Berlin, Germany

**ABSTRACT:** Molecular brush diblock copolymers were synthesized by the orthogonal overlay of the RAFT (reversible addition–fragmentation chain transfer), the ATRP (atom transfer radical polymerization), and the NMP (nitroxide-mediated polymerization) techniques. This unique combination enabled the synthesis of the complex amphiphilic polymers without the need of postpolymerization modifications, using a diblock copolymer intermediate made from two selectively addressable inimers and applying a sequence of four controlled free radical polymerization steps in total. The resulting polymers are composed of a thermosensitive poly(*N*-isopropylacrylamide) brush as hydrophilic block and a polystyrene brush as hydrophobic block, thus translating the structure of the established amphiphilic diblock copolymers known as macro surfactants to the higher size level of “giant surfactants”. The dual molecular brushes and the aggregates formed on ultra flat solid substrates were visualized by scanning force microscopy (SFM).



## INTRODUCTION

The strive for increasingly complex polymer architectures has gained much impetus by the advent of the so-called controlled radical polymerization (CRP) methods,<sup>1–4</sup> now by IUPAC named reversible-deactivation radical polymerization (RDRP).<sup>5</sup> For instance, amphiphilic linear multiblock, graft, and star copolymers that self-organize into a wealth of mesoscopic structures have become accessible starting from a large selection of monomers.<sup>6</sup> An intriguing recent development are dual bottle brush block copolymers, i.e., heterografted brush block copolymers, bearing densely grafted hydrophilic and hydrophobic linear side chains on the polymeric backbone. Such blocky “molecular bottle brushes”<sup>7–9</sup> are e.g. of interest for nanostructured materials with large domain spacings<sup>10–12</sup> or as novel “giant” surfactants.<sup>13–16</sup> Still, their synthesis is painstaking. Instead of “grafting onto” processes with all their inherent problems,<sup>16</sup> two more efficient strategies to dual bottle brush block copolymers have been conceived: the block copolymerization of hydrophilic and hydrophobic macromonomers and orthogonal “grafting from” strategies (Scheme 1). However, due to the inherent difficulties to control the radical polymerization of vinyl macromonomers, the former strategy has been mostly limited to poly(norbornene) backbones with longer ( $C_5$ ) repeat units so far to achieve high degrees of polymerization.<sup>10,17–19</sup> An additional drawback arises from the poor miscibility of hydrophilic and hydrophobic macromonomers. The “grafting from” strategy has thus been favored, combining different methods of controlled polymerization, such as ring-opening polymerization (ROP) and CRP methods, as e.g. atom transfer polymerization (ATRP) or reversible addition–fragmentation chain transfer (RAFT).<sup>8,9,12,13,20,21</sup> Despite impressive results, these approaches have been restricted by the limited choice of monomers suited for ROP and the frequent

need of protective group chemistry.<sup>9,11,12,19,22,23</sup> Recently, truly amphiphilic dual bottle brushes were made by combining the macromonomer and the “grafting from” strategies, while superposing two CRP methods, either RAFT and ATRP or RAFT and nitroxide-mediated polymerization (NMP), without the need of protective group chemistry or of additional chemical modifications.<sup>14,15</sup> Here, we demonstrate that it is possible to push this most direct approach even further. Employing orthogonally the three best established CRP methods, namely RAFT, ATRP, and NMP, in one single synthetic sequence, we exemplify the enormous potential of combining CRP methods in the straightforward design of complex macromolecular structures. In the particular case, we synthesized dual bottle brushes, consisting of a hydrophobic polystyrene brush, and a hydrophilic, thermosensitive poly(*N*-isopropylacrylamide) brush. Such giant amphiphiles correspond to the structure of the well-known thermosensitive poly(styrene-*block-N*-isopropylacrylamide) copolymer surfactants.<sup>24–28</sup>

## EXPERIMENTAL SECTION

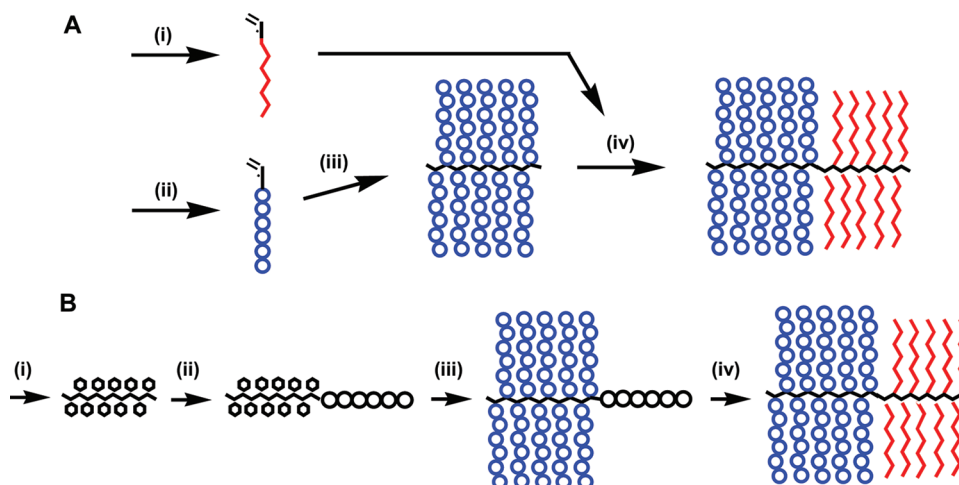
**Materials.** Styrene (Aldrich, 99%) was distilled in vacuo. *N*-Isopropylacrylamide (NIPAM) was precipitated from methanol to remove the inhibitor prior to polymerization. 2,2'-Azobis(isobutyronitrile) (AIBN, Acros-Organics, 98%) was crystallized from methanol and dried in vacuo. All solvents used for polymerization and purification were analytical grade and used as received. Zellu-Trans dialysis tubes (nominal molar mass cutoff of 4000–6000 Da) were from Roth. The synthesis of RAFT agent 4-(trimethylsilyl)benzyl 4'-(trimethylsilyl)butanedithioate (CTA1),<sup>29</sup> inimer

**Received:** July 8, 2011

**Revised:** November 5, 2011

**Published:** November 22, 2011

**Scheme 1. Synthetic Strategies to Amphiphilic Dual Bottle Brush Block Copolymers: (A) Block Copolymerization of Prefabricated Macromonomers (“Grafting Through” Approach); (B) Block Copolymerization of Inimers Followed by Sequential Grafting Steps (“Grafting From” Approach)**



2-chloropropionyloxyethyl acrylate (CIPEA),<sup>15</sup> inimer 2-phenyl-2-(2,2,6,6-tetramethyl-piperidine-1-oxyl)ethyl acrylate ( $\Phi$ TEA),<sup>14</sup> and tris[2-(dimethylamino)ethyl]amine ( $\text{Me}_6\text{TREN}$ )<sup>30</sup> was reported before.

**Polymer Synthesis.** *Synthesis of ( $\Phi$ TEA)<sub>96</sub>.* In a typical procedure, a mixture of  $\Phi$ TEA (1.8 g,  $5.6 \times 10^{-3}$  mol), CTA1 (10 mg,  $2.8 \times 10^{-5}$  mol), and AIBN (0.9 mg,  $5.6 \times 10^{-6}$  mol) in dry THF (2 mL) was degassed by three freeze–pump–thaw cycles, sealed, and placed in an oil bath at 65 °C. After 60 h, the reaction was stopped by cooling and precipitated two times into methanol to give the polymer ( $\Phi$ TEA)<sub>96</sub> (0.5 g).  $M_n^{\text{theor}} = 25$  kg/mol. SEC (RI detector):  $M_n^{\text{SEC}} = 3.3$  kg/mol,  $M_w/M_n = 1.5$ . <sup>1</sup>H NMR (300 MHz,  $\text{CDCl}_3$ ):  $M_n^{\text{NMR}} = 42$  kg/mol, Z/R = 0.8. <sup>1</sup>H NMR (300 MHz,  $\text{CDCl}_3$ ):  $\delta_{\text{H}} = 0.01$  (TMS<sub>Z</sub> group), 0.26 (TMS<sub>R</sub> group), 0.65, 1.02, 1.17, 1.33, 1.47 (5 × br s, TEMPO moiety), 1.87 (br s, –CH– backbone), 4.11 (br s, 1 H), 4.57 (br s, 1 H), 4.88 (br s, 1 H), 7.24 (br s, 5 H).

*Synthesis of ( $\Phi$ TEA)<sub>96</sub>-b-(CIPEA)<sub>359</sub>.* In a typical procedure, a mixture of CIPEA (0.38 g,  $1.8 \times 10^{-3}$  mol), ( $\Phi$ TEA)<sub>96</sub> (0.3 g,  $M_n^{\text{NMR}} = 32$  kg/mol,  $9.3 \times 10^{-6}$  mol), and AIBN (0.15 mg,  $9.3 \times 10^{-7}$  mol) in dry benzene (1.5 mL) was degassed by three freeze–pump–thaw cycles, sealed, and placed in an oil bath at 65 °C. After 14 h, the reaction was stopped by cooling and precipitated twice into methanol and twice into hexane to give the purified block copolymer ( $\Phi$ TEA)<sub>96</sub>-b-(CIPEA)<sub>359</sub> (yield: 0.3 g). SEC (RI detector):  $M_n^{\text{theor}} = 62$  kg/mol.  $M_n^{\text{SEC}} = 20$  kg/mol,  $M_w/M_n = 1.5$ . <sup>1</sup>H NMR (300 MHz,  $\text{CDCl}_3$ ):  $M_n^{\text{NMR}} = 105$  kg/mol, Z/R = 0. <sup>1</sup>H NMR (300 MHz,  $\text{CDCl}_3$ ):  $\delta_{\text{H}} = 0.64$ , 1.01, 1.16, 1.33, 1.48 (5 × br s, TEMPO moiety), 1.64 (br d,  $J = 6.84$  Hz,  $\text{ClCHCH}_3$ ), 1.95 (br s, –CH<sub>2</sub>– backbone), 2.35 (br s, –CH– backbone), 4.12 (br s, 1 H), 4.30 (br s, 2 H), 4.37 (br s, 2 H), 4.47 (br q,  $J = 6.84$  Hz,  $\text{ClCHCOO}$ –), 4.57 (br s, 1 H), 4.87 (br s, 1 H), 7.24 (br s, 5 H).

*Synthesis of ( $\Phi$ TEA)<sub>96</sub>-b-(CIPEA-g-NIPAM)<sub>50</sub>359.* In a typical procedure, macroinitiator ( $\Phi$ TEA)<sub>96</sub>-b-(CIPEA)<sub>359</sub> (50 mg,  $M_n^{\text{NMR}} = 105$  kg/mol, corresponds to  $1.7 \times 10^{-4}$  mol initiating Cl groups) was dissolved in ethyl acetate (4.75 g) and CuCl (16.7 mg,  $1.7 \times 10^{-4}$  mol), NIPAM (3.8 g, 33 mmol), and iPrOH (4.75 g) were added. The reaction mixture was purged with argon for 30 min, tris[2-(dimethylamino)ethyl]amine  $\text{Me}_6\text{TREN}$  (39 mg,  $1.7 \times 10^{-4}$  mol) was added, and the mixture was polymerized at 25 °C for 3 h. The reaction was quenched by cooling, diluted, and dialyzed against deionized water (dialysis membranes Zellu-Trans from Roth (Germany), nominal cutoff 4000–6000). Finally, the aqueous polymer solution is lyophilized and dried under high vacuum to

obtain ( $\Phi$ TEA)<sub>96</sub>-b-(CIPEA-g-NIPAM)<sub>50</sub>359 (yield: 1 g).  $M_n^{\text{theor}} = 2135$  kg/mol. SEC (RI detector):  $M_n^{\text{SEC}} = 133$  kg/mol,  $M_w/M_n = 1.6$ . The average length of the NIPAM grafts was calculated from the amount of NIPAM incorporated and the number of initiating sites per macroinitiator.

The synthesis of ( $\Phi$ TEA)<sub>96</sub>-b-(CIPEA-g-NIPAM)<sub>44</sub>359 followed the same protocol except for that the amounts of CuCl (8.3 mg,  $8.45 \times 10^{-5}$  mol) and  $\text{Me}_6\text{TREN}$  (19 mg,  $8.45 \times 10^{-5}$  mol) were reduced. Finally, the same work-up yielded ( $\Phi$ TEA)<sub>96</sub>-b-(CIPEA-g-NIPAM)<sub>44</sub>359 (yield: 0.83 g). SEC (RI detector):  $M_n^{\text{SEC}} = 114$  kg/mol,  $M_w/M_n = 1.4$ . <sup>1</sup>H NMR (300 MHz,  $\text{CDCl}_3$ ):  $\delta_{\text{H}} = 1.15$  (br s,  $\text{CH}(\text{CH}_3)_2$ ), 1.64 (br s, –CH<sub>2</sub>– backbone), 1.83 (br s, –CH<sub>2</sub>– backbone), 2.12 (br s, –CH– backbone), 4.00 (br s,  $\text{CH}(\text{CH}_3)_2$ ), 6.36 (br s, NH).

*Synthesis of ( $\Phi$ TEA-g-PS)<sub>64</sub>96-b-(CIPEA-g-NIPAM)<sub>50</sub>359.* In a typical procedure, macroinitiator ( $\Phi$ TEA)<sub>96</sub>-b-(CIPEA-g-NIPAM)<sub>50</sub>359 (0.200 g,  $M_n^{\text{theor}} = 2130$  kg/mol, corresponds to  $8.9 \times 10^{-6}$  mol initiating TEMPO groups) was dissolved in DMAc (2 mL). After the macroinitiator was homogeneously dissolved, styrene (340 mg,  $1.7 \times 10^{-3}$  mol) was added to the solution. The mixture was degassed by three freeze–pump–thaw cycles, sealed, and placed in an oil bath at 135 °C. After 13 h, the reaction was quenched by cooling and precipitated into diethyl ether. The polymer was isolated and dried in vacuo to yield the dual brush block copolymer ( $\Phi$ TEA-g-PS)<sub>64</sub>96-b-(CIPEA-g-NIPAM)<sub>50</sub>359 (yield: 200 mg).  $M_n^{\text{theor}} = 2130$  kg/mol. SEC (RI detector):  $M_n^{\text{SEC}} = 125$  kg/mol,  $M_w/M_n = 1.7$ .  $M_n^{\text{NMR}} = 2850$  kg/mol.

The synthesis of ( $\Phi$ TEA-g-PS)<sub>116</sub>96-b-(CIPEA-g-NIPAM)<sub>44</sub>359 was carried out analogously. Macroinitiator ( $\Phi$ TEA)<sub>96</sub>-b-(CIPEA-g-NIPAM)<sub>44</sub>359 (0.200 g,  $M_n^{\text{theor}} = 1890$  kg/mol, corresponds to  $10 \times 10^{-6}$  mol initiating TEMPO groups) was dissolved in NMP (4 mL). After the macroinitiator was homogeneously dissolved, styrene (410 mg,  $4 \times 10^{-3}$  mol) was added to the solution, and the mixture was degassed by three freeze–pump–thaw cycles, sealed, and placed in an oil bath at 135 °C. After 21 h, the reaction was quenched by cooling and precipitated into diethyl ether. The polymer was isolated and dried in vacuo to yield the dual brush block copolymer ( $\Phi$ TEA-g-PS)<sub>116</sub>96-b-(CIPEA-g-NIPAM)<sub>44</sub>359 (yield: 200 mg).  $M_n^{\text{theor}} = 3050$  kg/mol. SEC (RI detector):  $M_n^{\text{SEC}} = 118$  kg/mol,  $M_w/M_n = 1.4$ .  $M_n^{\text{NMR}} = 3440$  kg/mol. <sup>1</sup>H NMR (300 MHz,  $\text{CDCl}_3$ ):  $\delta_{\text{H}} = 1.14$  (br s,  $\text{CH}(\text{CH}_3)_2$ ), 1.41 (br s, –CH<sub>2</sub>– backbone), 1.84 (br s, –CH<sub>2</sub>– backbone), 2.09 (br s, –CH– backbone), 4.00 (br s,  $\text{CH}(\text{CH}_3)_2$ ), 6.58 (br m, styrene), 7.06 (br s, styrene). The average length of the PS grafts was calculated from

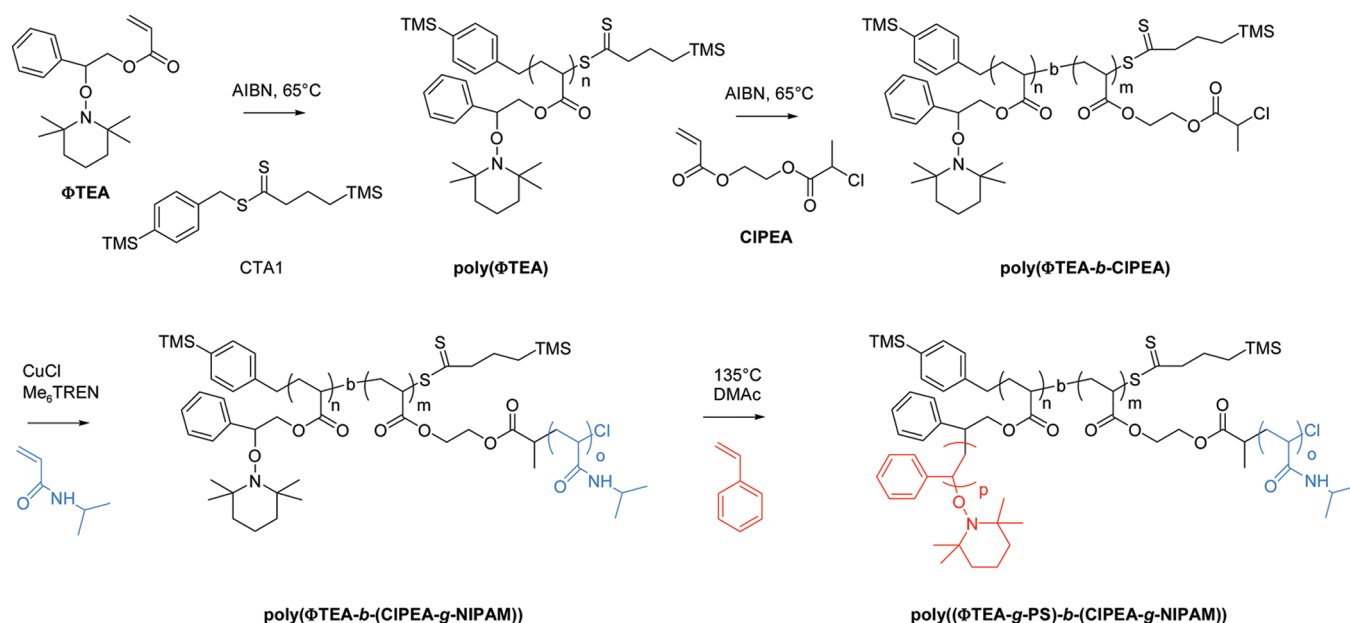


**Figure 1.** Synthesis of the amphiphilic dual brush block copolymers  $\text{poly}((\Phi\text{TEA-g-PS})-b\text{-(CIPEA-g-NIPAM)})$  by subsequent RAFT, ATRP, and NMP polymerizations.

the amount of styrene incorporated and the number of initiating sites per macroinitiator.

**Methods.** SEC analysis of both  $(\Phi\text{TEA})_{96}$  and  $(\Phi\text{TEA})_{96}\text{-}b\text{-(CIPEA)}_{359}$  was carried out at 25 °C in THF (flow rate: 1.0 mL/min) using a TSP apparatus (Thermo Separation Products from Thermo-Finnigan GmbH, Dreieich, Germany) equipped with a Shodex RI-71 refractive index detector, a TSP UV detector (260 nm), and a set of PSS SDV columns (styrene/divinylbenzene, 1000 and 10 000 Å porosity, 5  $\mu\text{m}$  particle size). Calibration was performed with polystyrene standards (PSS GmbH Mainz, Germany). SEC analysis of the polymers  $\text{poly}(\Phi\text{TEA})\text{-}b\text{-(CIPEA-g-NIPAM)}$  and  $\text{poly}(\Phi\text{TEA-g-PS})\text{-}b\text{-(CIPEA-g-NIPAM)}$  were carried out at 25 °C in NMP with 0.05 M LiBr (flow rate: 0.5 mL/min) using a TSP apparatus (Thermo Separation Products from Thermo-Finnigan GmbH, Dreieich, Germany) equipped with a Shodex RI-71 refractive index detector, a TSP UV detector (270 nm), and a set of PSS SDV columns (polyester, 100 and 1000 Å porosity, 7  $\mu\text{m}$  particle size). Calibration was performed with polystyrene standards (PSS GmbH Mainz, Germany).  $^1\text{H}$  and  $^{13}\text{C}$  NMR spectra were taken with a Bruker Avance 300 apparatus. All spectra are referenced to the solvent residual peak ( $\text{CHCl}_3$  at 7.26 ppm). The conversions of all polymerizations were measured before work-up by comparing the intensity of the vinyl proton signals with the intensity of characteristic signals of the polymers.

For scanning force microscopy (SFM), a droplet of a solution of the polymer in  $\text{CHCl}_3$  (0.01 g  $\text{L}^{-1}$ ) was deposited on a freshly cleaved mica surface and spun off after 5 s. The surface was dried under a flux of nitrogen gas and then imaged by SFM in tapping-mode under ambient conditions. As apparatus, Nanoscope 3a (Veeco) was employed using silicon cantilevers (Olympus, Japan) with a typical resonance frequency of 300 kHz and a spring constant of about 42 N  $\text{m}^{-1}$ . Both height and phase images were recorded.

## RESULTS AND DISCUSSION

At the heart of our synthetic approach are specialty monomers, so-called inimers, that bear simultaneously a polymerizable and an initiating group. Originally conceived for the preparation of hyperbranched polymers,<sup>31,32</sup> the controlled linear

homopolymerization of inimers via RAFT without affecting the initiating sites was shown recently.<sup>11,12,14,15</sup> In this way, homopolymers densely functionalized with initiating sites are accessible, which can be subsequently activated via CRP methods (Scheme 1). Thus, the block copolymerization of two inimers with different, orthogonally addressable initiating sites, to be followed by selective grafting polymerization steps, provides a versatile approach to amphiphilic dual bottle brushes.

Hence, we designed the model polymer  $\text{poly}((\Phi\text{TEA-g-PS})\text{-}b\text{-(CIPEA-g-NIPAM)})$  with a polyacrylate backbone, a hydrophobic block made of polystyrene (PS), and a hydrophilic block made of the thermosensitive poly(*N*-isopropylacrylamide) (NIPAM) as heterografted brush building blocks. The synthetic route comprises four consecutive CRP steps (Figure 1): Initially, inimers  $\Phi$ TEA and CIPEA are block copolymerized by the RAFT method to give  $\text{poly}(\Phi\text{TEA}-b\text{-CIPEA})$  carrying complementary orthogonal initiating sites. This intermediate is transformed into an amphiphilic dual bottle brush by two sequential “grafting from” steps using NIPAM and styrene via ATRP and NMP, respectively. While the two initial polymerizations could be conducted under standard RAFT conditions, the ATRP grafting step needed the presence of the strongly activating ligand tris[2-(dimethylamino)ethyl]amine ( $\text{Me}_6\text{TREN}$ ), and the NMP grafting step required the additional solvent *N,N*-dimethylacetamide (DMAc) to provide homogeneous polymerization conditions. As size exclusion chromatography (SEC) for such complex polymers can only give approximate data, we employed a doubly trimethylsilyl (TMS)-labeled RAFT agent to support the characterization of the intermediate and final polymers.<sup>29,33,34</sup> Upon quantifying both polymer end groups of the linear polymer intermediates via the  $\text{TMS}_\text{R}$  and  $\text{TMS}_\text{Z}$  signals by  $^1\text{H}$  NMR spectroscopy, the absolute number-average molar mass  $M_n$  as well as the percentage of active end groups present after the first polymerization steps can be elucidated. The combined analytical data enabled us to determine the overall structure, composition, and molar mass of the various intermediates and the final amphiphilic dual brush block copolymers



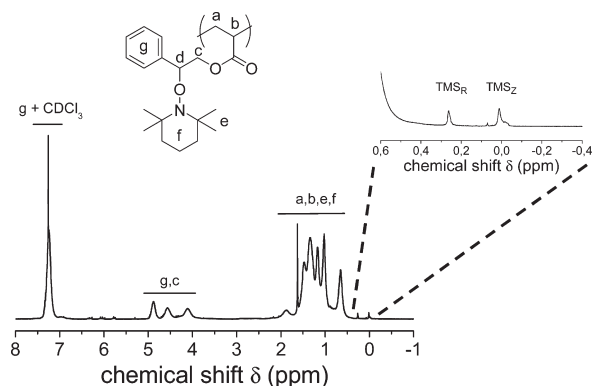


**Figure 2.**  $^1\text{H}$  NMR spectrum of  $(\Phi\text{TEA})_{96}$  in  $\text{CDCl}_3$ .  $\text{TMS}_\text{R}$  refers to aryl-bound TMS group (as part of the R group) of the RAFT agent;  $\text{TMS}_\text{Z}$  refers to the alkyl-bound TMS group (as part of the Z group).

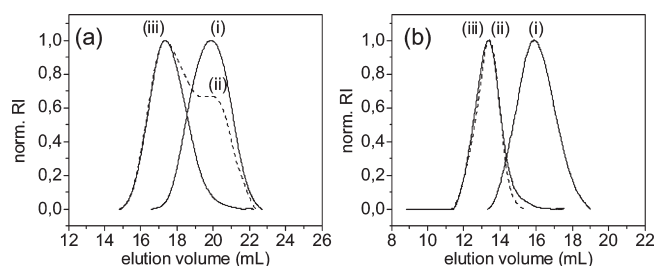


**Figure 3.** Size exclusion chromatography (SEC) analysis of a given polymer family. (a) SEC traces of  $(\Phi\text{TEA})_{96}$  (i, continuous line) and  $(\Phi\text{TEA})_{96}\text{-}b\text{-(CIPEA)}_{359}$  before (ii, dashed line) and after selective precipitation (iii, continuous line) in THF as eluent. (b) SEC traces of  $(\Phi\text{TEA})_{96}\text{-}b\text{-(CIPEA)}_{359}$  (i, continuous line),  $(\Phi\text{TEA})_{96}\text{-}b\text{-(CIPEA-g-(NIPAM)}_{50})_{359}$  (ii, dashed line), and  $(\Phi\text{TEA-g-(PS)}_{64})_{96}\text{-}b\text{-(CIPEA-g-(NIPAM)}_{50})_{359}$  (iii, continuous line) in NMP as eluent.

$(\Phi\text{TEA-g-(PS)}_{116})_{96}\text{-}b\text{-(CIPEA-g-(NIPAM)}_{44})_{359}$  and  $(\Phi\text{TEA-g-(PS)}_{64})_{96}\text{-}b\text{-(CIPEA-g-(NIPAM)}_{50})_{359}$ .

In the first polymerization step, the inimer  $\Phi\text{TEA}$  was polymerized by the RAFT method.  $^1\text{H}$  NMR analysis of the poly( $\Phi\text{TEA}$ ) exploiting the  $\text{TMS}_\text{R}$  and  $\text{TMS}_\text{Z}$  end groups, which were introduced into the polymer via the TMS-labeled RAFT agent CTA1 (see Figure 2), revealed a number-average degree of polymerization  $\text{DP}_\text{n}$  of 96 ( $M_\text{n}^\text{NMR} = 42 \text{ kg/mol}$ ), with a Z/R ratio of 80% ( $\text{TMS}_\text{Z}/\text{TMS}_\text{R} = 0.8$ ). This ratio suggested that 20% of the end groups of  $(\Phi\text{TEA})_{96}$  are cleaved off from the growing polymer chains during the RAFT process. We may speculate whether the relatively weak N—O—benzyl bond of the inimer repeat units, or steric demands due to their relative bulkiness in combination with the relatively bulky Z-group, give rise to some side reactions that reduce the fraction of active chain ends somewhat compared to optimized RAFT-made polymers.<sup>29</sup> But as generally, the percentage of active end groups for polymers made by RDRP is not verified, literature data for comparison are lacking. Nevertheless, SEC analysis of the polymer provided an apparent number-average molar mass  $M_\text{n}^\text{app}$  of 3.3 kg/mol, with a dispersity ( $M_\text{w}/M_\text{n}$ ) value of 1.5. The relatively narrow monomodal distribution of  $(\Phi\text{TEA})_{96}$  seen in the SEC elugrams (Figure 3a) thus supports the controlled polymerization of  $(\Phi\text{TEA})_{96}$ .

Subsequently, homopolymer  $(\Phi\text{TEA})_{96}$  was used as macro-RAFT agent in the polymerization of the inimer CIPEA. As the quality of  $(\Phi\text{TEA})_{96}$  was only moderate ( $\text{TMS}_\text{Z}/\text{TMS}_\text{R} = 0.8$ ),

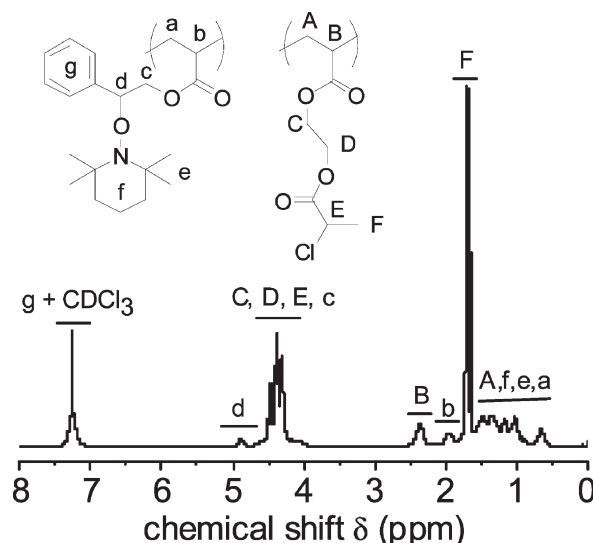


**Figure 4.**  $^1\text{H}$  NMR spectrum of  $(\Phi\text{TEA})_{96}\text{-}b\text{-(CIPEA)}_{359}$  in  $\text{CDCl}_3$ .

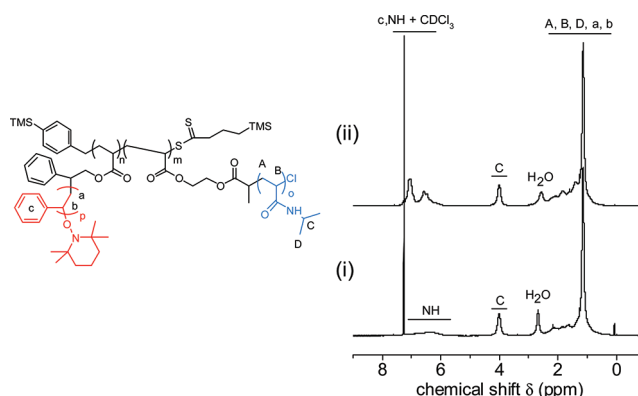


**Figure 5.**  $^1\text{H}$  NMR spectra in  $\text{CDCl}_3$ : (i)  $(\Phi\text{TEA})_{96}\text{-}b\text{-(CIPEA-g-(NIPAM)}_{50})_{359}$ ; (ii)  $(\Phi\text{TEA-g-(PS)}_{64})_{96}\text{-}b\text{-(CIPEA-g-(NIPAM)}_{50})_{359}$ .

it is not surprising that the SEC elugram of the crude reaction product was bimodal (Figure 3a). Still, selective precipitation provided the pure block copolymer poly( $\Phi\text{TEA-b-CIPEA}$ ) with a monomodal molar mass distribution (Figure 3a), with  $M_\text{n}^\text{app} = 20 \text{ kg/mol}$  and dispersity ( $M_\text{w}/M_\text{n}$ ) = 1.5.  $^1\text{H}$  NMR spectra confirmed the successful synthesis of the block copolymer, with the characteristic proton resonances of both  $\Phi\text{TEA}$  and CIPEA being well resolved (Figure 4). Importantly, the proton patterns of both blocks are distinguishable, indicating the stability of the initiating sites in the side chains during the RAFT process. From the  $^1\text{H}$  NMR analysis, the actual composition of the block copolymer is calculated as  $(\Phi\text{TEA})_{96}\text{-}b\text{-(CIPEA)}_{359}$  ( $M_\text{n}^\text{NMR} = 105 \text{ kg/mol}$ ). Thus, the RAFT process proved to be a tolerant method to create highly functionalized block copolymers with differently addressable initiating sites for further “grafting from” steps.

In the third step, the pendant chlorine substituents of the  $(\text{CIPEA})_{359}$  block were used to initiate selectively the controlled ATRP polymerization of NIPAM. In order to suppress possible side reactions of the nitroxylamine groups, the ATRP polymerization was carried out at 25 °C. Accordingly, the catalyst system  $\text{Me}_6\text{TREN}$  and  $\text{CuCl}$  was applied in 2-propanol to control the first “grafting from” step, as such conditions in combination with

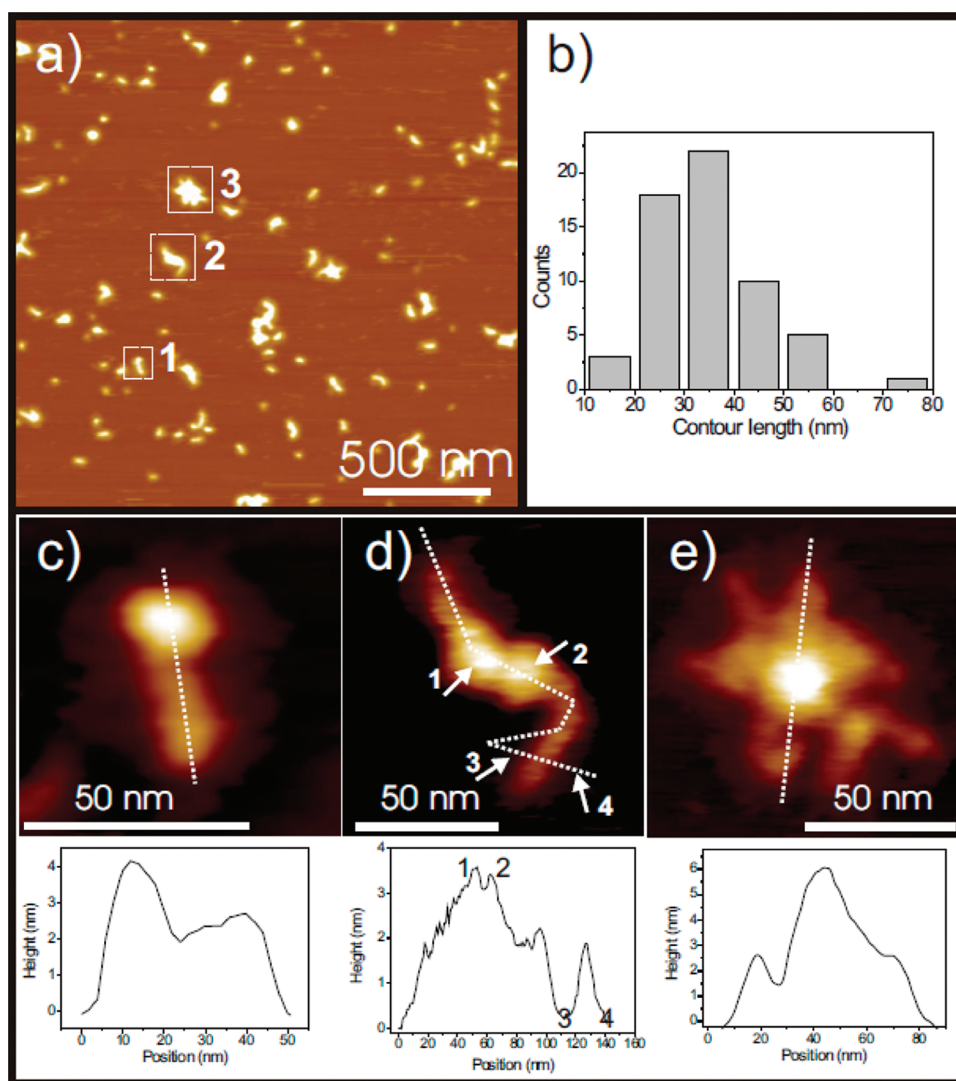


**Figure 6.** (a) SFM height image of  $(\Phi\text{TEA-g-(PS)}_{116})_{96}\text{-b-(CIPEA-g-(NIPAM)}_{44})_{359}$  deposited on mica by spin-coating from  $\text{CHCl}_3$  solution. (b) Histogram of measured contour lengths of single molecules. Zoom-in on (a): (c) single molecule 1, (d) dimer 2, and (e) oligomer 3, including their height profile cross sections.

the use of chloride initiators, as present in the CIPEA reat units, have been shown to give best control over ATRP of acrylamide monomers, specifically of NIPAM.<sup>35–37</sup> Figure 5 (see spectrum i) shows a corresponding  $^1\text{H}$  NMR spectrum with the characteristic NIPAM signals. This indicated the successful first “grafting from” step, namely of NIPAM, to provide  $(\Phi\text{TEA})_{96}\text{-b-(CIPEA-g-(NIPAM)}_{50})_{359}$ . As to be expected, the proton resonances of the poly $\Phi\text{TEA}$  block are no more resolved because the molar fraction of the  $\Phi\text{TEA}$  repeat units in  $(\Phi\text{TEA})_{96}\text{-b-(CIPEA-g-(NIPAM)}_{50})_{359}$  amounts only to 1 wt %. The monomodal distributed SEC elugram, which is clearly shifted in comparison to the elugram of the precursor polymer, corroborated the successful grafting of the hydrophilic NIPAM brush arms (Figure 3b), with  $M_n^{\text{app}} = 133$  kg/mol and dispersity ( $M_w/M_n$ ) = 1.6. Additionally, the sample  $(\Phi\text{TEA})_{96}\text{-b-(CIPEA-g-(NIPAM)}_{44})_{359}$  was synthesized by the same protocol except for the ratio of the chlorine initiating sites to  $\text{CuCl}$ , which was reduced in order to increase the grafting density of the growing side chains.<sup>38</sup> For the semibrush block copolymer, values of  $M_n^{\text{app}} = 114$  kg/mol and dispersity = 1.4 were found.

Finally, in the fourth CRP step, both semi bottle brushes  $(\Phi\text{TEA})_{96}\text{-b-(CIPEA-g-(NIPAM)}_{50})_{359}$  and  $(\Phi\text{TEA})_{96}\text{-b-(CIPEA-g-(NIPAM)}_{44})_{359}$  were destined as macroinitiators for the second “grafting from” reaction, the controlled polymerization of styrene via NMP. Because the macroinitiators were not soluble in styrene,  $N,N$ -dimethylacetamide (DMAc) was used as solvent to obtain homogeneous polymerization conditions. This is an indispensable prerequisite to guarantee the accessibility of the nitroxylamine groups in order to initiate the second “grafting from” process evenly. Figure 5 (see spectrum ii) shows the  $^1\text{H}$  NMR spectrum of the purified polymer. The characteristic proton signal pattern of polystyrene PS in addition to the characteristic NIPAM signals already present in the precursor indicates the successful polymerization of styrene. Assuming that all polystyrene grafts were successfully covalently attached to the  $(\Phi\text{TEA})_{96}\text{-b-(CIPEA-g-(NIPAM)}_{50})_{359}$  semibrush precursor, the actual composition of the dual bottle-brush polymers can be calculated as  $(\Phi\text{TEA-g-(PS)}_{64})_{96}\text{-b-(CIPEA-g-(NIPAM)}_{50})_{359}$ , with  $M_n^{\text{theo}} = 2130$  kg/mol and  $M_n^{\text{NMR}} = 2850$  kg/mol. The relatively narrow monomodal molar mass distribution of the final dual bottle-brush polymer is shown in Figure 3b ( $M_n^{\text{app}} = 125$  kg/

mol (calibration with polystyrene standard)s and dispersity ( $M_w/M_n = 1.7$ ). Noteworthy, no shift to lower elution volumes was observed in comparison to the semibrush precursor. Analogously, the narrowly distributed ( $\Phi$ TEA-*g*-(PS)<sub>116</sub>)<sub>96</sub>-*b*-(CIPEA-*g*-(NIPAM)<sub>44</sub>)<sub>359</sub> was synthesized (with  $M_n^{\text{theo}} = 3050$  kg/mol,  $M_n^{\text{NMR}} = 3440$  kg/mol,  $M_n^{\text{app}} = 118$  kg/mol, dispersity ( $M_w/M_n = 1.4$ ), showing the analogous elution behavior as its homologue described above. Apparently, the additional polystyrene side chains do not increase the hydrodynamic volume of the dual brush block copolymers notably compared to the precursor semibrushes. This may be understood as the contour length is only weakly changed by the second “grafting from” step, and thus both ( $\Phi$ TEA-*g*-(PS)<sub>64</sub>)<sub>96</sub>-*b*-(CIPEA-*g*-(NIPAM)<sub>50</sub>)<sub>359</sub> and ( $\Phi$ TEA)<sub>96</sub>-*b*-(CIPEA-*g*-(NIPAM)<sub>44</sub>)<sub>359</sub> may be expected to elute at very close times. Most importantly, no additional peak at higher elution volumes was observed. This indicates the absence of lower molar mass contaminants, e.g., from the self-initiating polymerization of styrene.<sup>14</sup> Nevertheless, it is clear that the grafting efficiencies for neither the hydrophilic nor the hydrophobic block can be 100% (see discussion below),<sup>38</sup> and thus, the true lengths of the graft arms are longer than the formally calculated average values.

Scanning force microscopy (SFM) provided further proof for the successful synthesis of the structural dual brush motif. An exemplary SFM image of ( $\Phi$ TEA-*g*-(PS)<sub>116</sub>)<sub>96</sub>-*b*-(CIPEA-*g*-(NIPAM)<sub>44</sub>)<sub>359</sub> adsorbed on mica is shown in Figure 6a. The small-sized objects are attributed to single molecules and to aggregates thereof. The distribution of the contour lengths of single molecules reveals a number-averaged length  $L_n = 33$  nm (Figure 6b). Zooming in onto a single molecule reveals a “tadpole-like” structure, with a relatively large “head” and a long “tail” (Figure 6c). A cross section through the height profile along the molecular backbone reveals a height difference between the head (4.2 nm) and the tail (2.6 nm). Similar heights were observed in the profile of a dimer formed by two molecules positioned head-to-head (Figure 6d). “Flowerlike” oligomers, also formed by a head-to-head manner, exhibited a higher head (6.1 nm) but a similar height of the tail compared with single molecules (Figure 6e). The average full width of the tail is around 21 nm (Figure 6d), taking into account a tip broadening effect<sup>39</sup> on the order of 4 nm, upon assuming a tip radius of 7 nm and an average height of the tail (spine and corona) around 1 nm.

Previously,<sup>40</sup> the formation of a tadpole structure was observed for a brush polymer with a gradient of grafting density along the backbone, where the single molecules were incorporated in a condensed monolayer. The tadpole formation was attributed to the compression, upon which the end with the higher grafting density forms the head.

Here, we attribute the formation of isolated tadpole structures for one amphiphilic block copolymer molecule to the differences in the chemical structure of both blocks, in side chain lengths, as well as in the different wetting behaviors of both blocks on the surface.<sup>41</sup> During the drying phase, the hydrophilic NIPAM brush block favors contact with the polar mica surface, whereas the hydrophobic PS brush block minimizes the contact. Thus, after solvent evaporation, the NIPAM brush block is directly adsorbed on the mica surface, while the collapsed PS brush block is located on top of the polyNIPAM block. The longer hydrophilic block ( $N = 359$ ) with the shorter NIPAM side chains ( $N = 44$ ) forms the tail, while the shorter hydrophobic block ( $N = 96$ ) with the longer PS side chains ( $N = 116$ ) forms the spherical head. This picture is supported by the height and with cross-section analysis. The fully extended NIPAM block has a width of

22 nm ( $44 \times 2 \times 0.25$  nm), which is close to the experimental value of 21 nm. Our model agrees also with the work from Kumaki and Hashimoto, who showed that when a diblock copolymer PS-*b*-PMMA is deposited on a mica surface, the PS block collapses into a single PS coil on the top of PMMA chain.<sup>42</sup> Thus, the main chain of the brush structure is not fully stretched, but at least locally coiled. This explains the fact that the experimentally detected contour length (33 nm) is considerably shorter than the fully extended chain length ( $L_c = 455 \times 0.25$  nm = 113 nm for an all-trans conformation).

Alternatively, low initiating efficiencies have been put forward as rationale for apparently short contour lengths of cylindrical brushes on ultraflat solid substrates, reducing steric repulsion. Some reports showed that the “grafting from” method via ATRP had initiating efficiencies of about  $50 \pm 10\%$  and that the measured contour lengths of these cylindrical brushes were considerably shorter than theoretically expected for a stiff chain.<sup>38,43–45</sup> The calculated average lengths per repeat unit  $l$  were about 0.1 nm. This value is similar to our findings ( $l = 0.075$  nm). In fact, considering our previously found grafting efficiencies of 50–80% for poly(CIPEA) as ATRP macroinitiator,<sup>15</sup> we can expect also in the present case a grafting efficiency within the same range for the hydrophilic NIPAM brush block, in agreement with the observed contour length.

The formation of “head and tail” conformation is also supported by looking into the length of the side chains. When the side chains are shorter than the polymer backbone, polymer brushes exhibit a cylindrical conformation, while in the opposite case, other conformations such as “starlike” conformation are formed.<sup>8,46,47</sup> In our particular case, the NIPAM side chains ( $N = 44$ ) are shorter than the backbone ( $N = 359$ ), thus forming the cylindrical “tail”, while the PS side chains ( $N = 116$ ) are longer than the backbone ( $N = 96$ ), thus favoring a spherical “head”. Finally, the formation of dimers and oligomers may be attributed to hydrophobic interactions between the PS brush blocks.<sup>42</sup>

## CONCLUSIONS

All the three most frequently applied CRP methods, namely RAFT, ATRP, and NMP, can be applied orthogonally and thus combined into one single synthetic sequence. This powerful approach enables the straightforward synthesis of complex polymer architectures starting from monomers, in a minimum number of reactions, and without the need of any postpolymerization modification step. The approach was exemplified by the synthesis of new high molar mass amphiphilic brush block copolymers consisting of polystyrene and poly(NIPAM) molecular brushes. The heterografted structure of these giant amphiphiles was characterized by SFM studies on the single molecular level.

## AUTHOR INFORMATION

### Corresponding Author

\*E-mail: laschews@rz.uni-potsdam.de.

## ACKNOWLEDGMENT

We thank M. Gräwert and H. Schlaad (Max-Planck-Institut for Colloids and Interfaces, Potsdam-Golm) for SEC measurements, A. Krititschka and M. Heydenreich (University of Potsdam) for NMR measurements, and J.-F. Lutz (Fraunhofer IAP, Potsdam-Golm) and M. Gradzielski (Technische Universität Berlin) for fruitful discussions. Financial support was given by Deutsche



Forschungsgemeinschaft DFG (Sfb 448 and Sfb765) and by Fonds der Chemischen Industrie.

## REFERENCES

- (1) Colombani, D. *Prog. Polym. Sci.* **1997**, *22*, 1649–1720.
- (2) Moad, G.; Rizzardo, E.; Thang, S. H. *Acc. Chem. Res.* **2008**, *41*, 1133–1142.
- (3) Matyjaszewski, K.; Müller, A. H. E., Eds.; *Controlled and Living Polymerizations. From Mechanisms to Applications*; Wiley-VCH: Weinheim, 2009.
- (4) Ouchi, M.; Terashima, T.; Sawamoto, M. *Chem. Rev.* **2009**, *109*, 4963–5050.
- (5) Jenkins, A. D.; Jones, R. G.; Moad, G. *Pure Appl. Chem.* **2010**, *82*, 483–491.
- (6) Holder, S. J.; Sommerdijk, N. A. J. M. *Polym. Chem.* **2011**, *2*, 1018–1028.
- (7) Zhang, M.; Müller, A. H. E. *J. Polym. Sci., Part A: Polym. Chem.* **2005**, *43*, 3461–3481.
- (8) Sheiko, S. S.; Sumerlin, B. S.; Matyjaszewski, K. *Prog. Polym. Sci.* **2008**, *33*, 759–785.
- (9) Lee, H.-i.; Matyjaszewski, K.; Yu-Su, S.; Sheiko, S. S. *Macromolecules* **2008**, *41*, 6073–6080.
- (10) Runge, M. B.; Bowden, N. B. *J. Am. Chem. Soc.* **2007**, *129*, 10551–10560.
- (11) Rzaev, J. *Macromolecules* **2009**, *42*, 2135–2141.
- (12) Bolton, J.; Bailey, T. S.; Rzaev, J. *Nano Lett.* **2011**, *11*, 998–1001.
- (13) Cheng, Z.; Zhu, X.; Fu, G. D.; Kang, E. T.; Neoh, K. G. *Macromolecules* **2005**, *38*, 7187–7192.
- (14) Zehm, D.; Laschewsky, A.; Gradzielski, M.; Prévost, S.; Liang, H.; Rabe, J. P.; Schweins, R.; Gummel, J. *Langmuir* **2010**, *26*, 3145–3155.
- (15) Zehm, D.; Laschewsky, A.; Heunemann, P.; Gradzielski, M.; Prévost, S.; Liang, H.; Rabe, J. P.; Lutz, J.-F. *Polym. Chem.* **2011**, *2*, 137–147.
- (16) Lanson, D.; Schappacher, M.; Borsali, R.; Deffieux, A. *Macromolecules* **2007**, *40*, 9503–9509.
- (17) Xia, Y.; Olsen, B. D.; Kornfield, J. A.; Grubbs, R. H. *J. Am. Chem. Soc.* **2009**, *131*, 18525–18532.
- (18) Johnson, J. A.; Lu, Y. Y.; Burts, A. O.; Xia, Y.; Durrell, A. C.; Tirrell, D. A.; Grubbs, R. H. *Macromolecules* **2010**, *43*, 10326–10335.
- (19) Li, Z.; Ma, J.; Cheng, C.; Zhang, K.; Wooley, K. L. *Macromolecules* **2010**, *43*, 1182–1184.
- (20) Xie, M.; Dang, J.; Han, H.; Wang, W.; Liu, J.; He, X.; Zhang, Y. *Macromolecules* **2008**, *41*, 9004–9010.
- (21) Huang, K.; Rzaev, J. *J. Am. Chem. Soc.* **2009**, *131*, 6880–6885.
- (22) Ishizu, K.; Satoh, J.; Toyoda, K.; Sogabe, A. *J. Mater. Sci.* **2004**, *39*, 4295–4300.
- (23) Huang, K.; Canterbury, D. P.; Rzaev, J. *Macromolecules* **2010**, *43*, 6632–6638.
- (24) Cammas, S.; Suzuki, K.; Sone, C.; Sakurai, Y.; Kataoka, K.; Okano, T. *J. Controlled Release* **1997**, *48*, 157–164.
- (25) Nuopponen, M.; Ojala, J.; Tenhu, H. *Polymer* **2004**, *45*, 3643–3650.
- (26) Ray, B.; Isobe, Y.; Matsumoto, K.; Habaue, S.; Okamoto, Y.; Kamigaito, M.; Sawamoto, M. *Macromolecules* **2004**, *37*, 1702–1710.
- (27) Bivigou-Koumba, A. M.; Gornitz, E.; Laschewsky, A.; Müller-Buschbaum, P.; Papadakis, C. M. *Colloid Polym. Sci.* **2010**, *288*, 499–517.
- (28) Adelsberger, J.; Meier-Koll, A.; Bivigou-Koumba, A. M.; Busch, P.; Holderer, O.; Hellweg, T.; Laschewsky, A.; Müller-Buschbaum, P.; Papadakis, C. M. *Colloid Polym. Sci.* **2011**, *289*, 711–720.
- (29) Päch, M.; Zehm, D.; Lange, M.; Dambowsky, I.; Weiss, J.; Laschewsky, A. *J. Am. Chem. Soc.* **2010**, *132*, 8757–8765.
- (30) Ciampolini, M.; Nardi, N. *Inorg. Chem.* **1966**, *5*, 41–44.
- (31) Hawker, C. J.; Fréchet, J. M. J.; Grubbs, R. B.; Dao, J. *J. Am. Chem. Soc.* **1995**, *117*, 10763–10764.
- (32) Gaynor, S. G.; Edelman, S.; Matyjaszewski, K. *Macromolecules* **1996**, *29*, 1079–1081.
- (33) Marsat, J.-N.; Heydenreich, M.; Kleinpeter, E.; Laschewsky, A.; Berlepsch, H. v.; Böttcher, C. *Macromolecules* **2011**, *44*, xxx.
- (34) Weiss, J.; Laschewsky, A. *Langmuir* **2011**, *27*, 4465–4473.
- (35) Neugebauer, D.; Matyjaszewski, K. *Macromolecules* **2003**, *36*, 2598–2603.
- (36) Xia, Y.; Yin, X.; Burke, N. A. D.; Stöver, H. D. H. *Macromolecules* **2005**, *38*, 5937–5943.
- (37) Gao, Z.; Tao, X.; Cui, Y.; Satoh, T.; Kakuchi, T.; Duan, Q. *Polym. Chem.* **2011**, *2*, 2590–2596.
- (38) Neugebauer, D.; Sumerlin, B. S.; Matyjaszewski, K.; Goodhart, B.; Sheiko, S. S. *Polymer* **2004**, *45*, 8173–8179.
- (39) Butt, H.-J.; Guckenberger, R.; Rabe, J. P. *Ultramicroscopy* **1992**, *46*, 375–393.
- (40) Lord, S. J.; Sheiko, S. S.; LaRue, I.; Lee, H.-I.; Matyjaszewski, K. *Macromolecules* **2004**, *37*, 4235–4240.
- (41) Zhang, A.; Barner, J.; Gössl, I.; Rabe, J. P.; Schlüter, A. D. *Angew. Chem., Int. Ed.* **2004**, *43*, 5185–5188.
- (42) Kumaki, J.; Hashimoto, T. *J. Am. Chem. Soc.* **2003**, *125*, 4907–4917.
- (43) Xu, Y.; Bolisetti, S.; Drechsler, M.; Fang, B.; Yuan, J.; Ballauff, M.; Müller, A. H. E. *Polymer* **2008**, *49*, 3957–3964.
- (44) Xu, Y.; Yuan, J.; Müller, A. H. E. *Polymer* **2009**, *50*, 5933–5939.
- (45) Li, C.; Gunari, N.; Fischer, K.; Janshoff, A.; Schmidt, M. *Angew. Chem., Int. Ed.* **2004**, *43*, 1101–1104.
- (46) Dziezok, P.; Sheiko, S. S.; Fischer, K.; Schmidt, M.; Möller, M. *Angew. Chem., Int. Ed.* **1997**, *36*, 2812–2815.
- (47) Xu, Y.; Plamper, F.; Ballauff, M.; Müller, A. H. E. *Adv. Polym. Sci.* **2010**, *228*, 1–38.